J|A|C|S
COMMUNICATIONS

Published on Web 12/23/2006

A Complete Microfluidic Screening Platform for Rational Protein Crystallization

Billy T. C. Lau, Chris A. Baitz, Xiao P. Dong, and Carl L. Hansen*

Department of Physics and Astronomy, University of British Columbia, 6224 Agricultural Road, Vancouver, British Columbia V6T 1Z1, Canada

Received August 11, 2006; E-mail: chansen@phas.ubc.ca

By virtue of their unique mass transport properties, dense integration, and low reagent consumption, microfluidic devices have emerged as viable technologies for protein crystallization. Current microfluidic crystallization technologies have focused on two separate strategies: one using the large-scale integration of active microvalves,[1] and one using two-phase flows for the mixing and encapsulation of reagents.[2,3] Valved microfluidic systems for parallel control of large arrays of identical fluidic units have been successfully applied to the efficient screening and optimization of crystallization conditions by free interface diffusion.[4,5] Additionally, a microfluidic formulator device has been developed which uses computer control of integrated microvalves for programmable mixing and screening of arbitrary chemical formulations.[6] On-chip combinatorial mixing provides a powerful tool for screening applications where chemical composition must be optimized over a finite set of reagents and has been applied to systematic studies of protein phase space behavior prior to crystallization trials. However, due to the lack of long-term storage capability, the application of the formulator has thus far been restricted to assays with immediate optical readouts.

Two-phase microfluidic systems for screening crystallization conditions provide an elegant solution to assay storage, by both isolating chemical mixtures within nanoliter volume droplets and eliminating dispersion during droplet transport. These systems exploit a two-phase shear instability for the compartmentalization of reactions in an oil/water emulsion, allowing for rapid generation of nanoliter volume "plugs" and fast mixing by chaotic advection.[3,7,8] However, this mechanism of droplet formation provides restricted control over droplet chemistry, is compatible with only a small number of chemical inputs, and requires large volumes due to the continuous flow of the aqueous phase. Furthermore, droplet size, spacing, and frequency display a complex dependence on capillary number and hence on operating parameters including carrier and reagent viscosity, flow rate, channel dimensions, and surface tension.[9]

Here we describe a general microfluidic platform for large-scale screening of homogeneous assays that seamlessly integrates programmable serial mixing with high-density two-phase storage. The use of microvalves allows for the generation of single droplets at defined times, over a broad range of operating parameters and with precise and independent control over drop composition, size, and spacing. Arrays of chemically independent droplets are confined within a user-defined oil/water emulsion and stored at densities of approximately 1000 assays/cm^2. Long-term incubation and dynamic control over dehydration are achieved with a programmable "osmotic bath".[4] We demonstrate the use of this device as a complete platform for microfluidic protein crystallization by performing systematic studies of protein solubility behavior followed by nanoliter volume crystallization screening and optimization in vapor diffusion format.

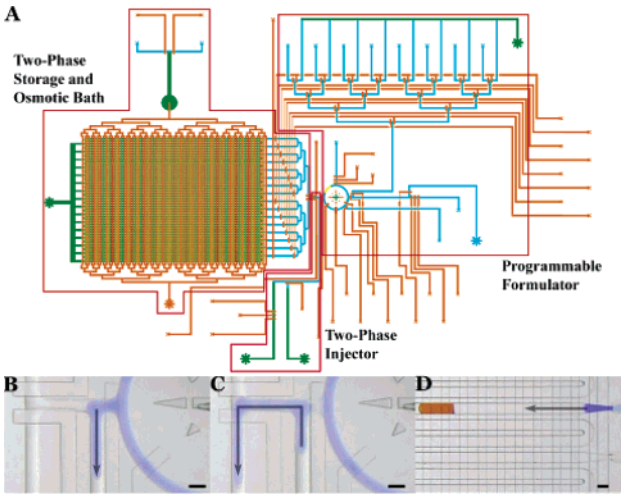

Figure 1. (A) Schematic of microfluidic screening platform. (B−C) Controlled two-step injection of an aqueous droplet (blue) into an immiscible carrier fluid (clear) using a peristaltic pump. (D) Delivery of a preformed droplet to selected section of the two-phase storage module formed by 16 addressable channels of square cross-section (100 μm × 100 μm). Scale bars are 100 μm.

Reagent mixing, droplet formation, and droplet incubation are accomplished on a single device consisting of three integrated modules: a formulation module, a droplet injector, and a two-phase storage module (Figure 1A). The formulator module creates programmed mixtures of stock reagents and protein sample within a 5 nL ring as previously described.[6] Once formed, protein mixtures may be imaged to determine the presence of aggregation and directed either to waste or to the two-phase storage module. The two-phase injector is used to create nanoliter volume droplets (Figure 1B,C) encapsulated in an immiscible carrier fluid consisting of a mixture of fluorocarbon oil (3M Fluorinert FC-70) and fluorous-soluble surfactant (DuPont ZONYL FSO-100).[10] Droplet formation using active microvalves and peristaltic pumps allows for complete control over droplet frequency, spacing, and volume, independent of capillary number and fluid properties (Figure 2A). Once formed, the droplets are directed through a bifurcated fluidic channel network to 1 of 16 sections of the storage array (Figure 1D). The partitioning of the array into 16 parallel channels mitigates the effect of pressure drops at each water-oil interface which otherwise limits the total number of droplets formed at a given pressure. A 1 cm^2 storage array filled with 400 2 nL droplets is shown in Figure 2B.

Long-term incubation and active control over reagent dehydration are achieved using a dynamic osmotic bath formed by a dense array of channels having a common inlet and outlet and separated from the storage array by a 25 μm thick gas-permeable membrane (Figure 1A).[4] Vapor transport proceeds until the vapor pressure of the reagents and the bath is equal. Periodic exchange of the osmotic

10.1021/ja065855b CCC: $37.00 © 2007 American Chemical Society

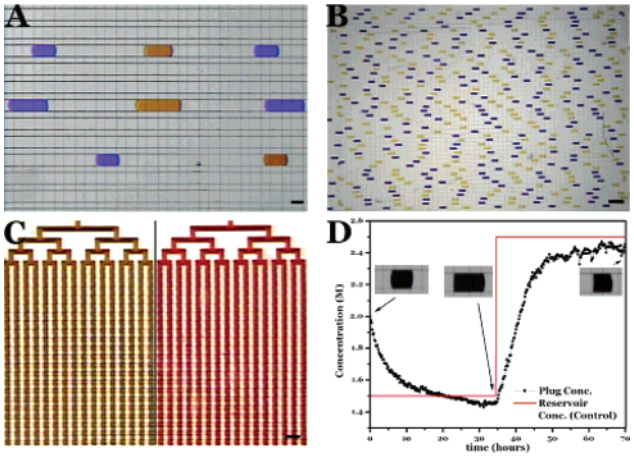

Figure 2. (A) Control over droplet size and spacing independent of viscosity. Blue droplets contain 4 mM bromophenol blue in 0.1 M Tris-HCl pH 8.5. Orange droplets contain 80% w/w glycerol with 1% w/w phenol red in 0.1 M Tris-HCl pH 8.5. Scale bar is 100 μm. (B) Four hundred 2 nL droplets stored in 10 mm × 7 mm section of an array. Droplets contain 4 mM bromophenol blue at pH 8.0 (blue) and 3.5 (yellow). (C) Control over osmotic bath using pulse-width modulation. Panel shows mixture of red and green dye at 100 ms cycle time, with red/green duty cycle percentages, respectively, at 75%/25% (left) and 25%/75% (right). Scale bar is 250 μm. (D) Dynamic and reversible control over droplet concentration (black) by pulse-width modulation of concentration in osmotic bath (red).

bath solution creates a boundary condition of well-defined vapor pressure, thereby setting the equilibrium osmotic strength of all the droplets. Dynamic control over this end point is achieved by pulse-width modulation of the flow between two reservoirs of high and low osmotic strength (Figure 2C). In addition to precise control of the equilibrium concentration, image analysis may be used to accurately monitor the size of droplets and the exact chemical concentrations over time (Figure 2D).

The microfluidic screening platform was used to implement a rational protein crystallization strategy in which systematic studies of the protein solubility are followed by nanoliter volume crystallization screening and optimization. Automated on-chip mixing of stock reagents was used to generate a four-dimensional solubility phase space for the protein catalase, with protein concentration, polyethylene glycol (PEG) molecular weight, PEG concentration, and pH as the independent variables. Phase mapping was performed using an efficient search algorithm, based on real-time image analysis and feedback, to adjust protein and PEG concentrations in order to track the solubility boundary. A total of 20 two-dimensional projections of phase space, with fixed pH and PEG molecular weight, were generated (Figure 3A).

Experimentally determined solubility curves were used to select 40 crystallization conditions lying just within the solubility region. All conditions were set on a single device, and stepwise increases in the osmotic bath strength were then used to concentrate the reactions, causing them to enter a region of supersaturation (Figure 3B). Droplets were observed initially and after equilibration with two bath conditions: 1 M NaCl and 2 M NaCl; 31 of 40 conditions produced crystals at 1 M NaCl, and all conditions formed crystals against a 2 M NaCl osmotic bath.

We further implemented a systematic protocol determining crystallization conditions using real-time feedback of protein solubility. A single device was used for the sequential titration of four model proteins (catalase, glucose isomerase, thaumatin, and ferritin) with increasing concentration of crystallization agent until aggregation was detected. Subsequent dilution with water was then carried out until the aggregate re-dissolved and the protein mixtures were stored in droplets for equilibration against the osmotic bath.

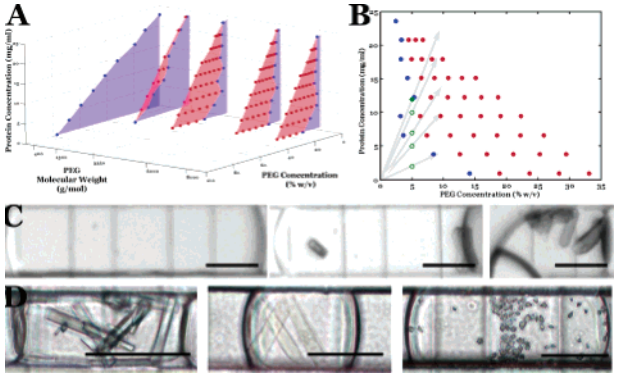

Figure 3. Rational protein crystallization strategy. (A) Three-dimensional projection of phase space for catalase with PEG molecular weight, PEG concentration, and protein concentration varied at constant pH (Tris 7.5). Plot shows boundary of aggregation region (red) and soluble region (blue). (B) Two-dimensional phase space for catalase at pH 7.5 with PEG 8000 as precipitant. Five crystallization trials (green) were chosen to lie just inside the soluble region. Arrows show the evolution of experiments during stepwise dehydration. (C) Micrographs of a crystallization trial from (B) showing droplet concentration and resulting crystal growth. Images are taken immediately after droplet formation (left), in equilibrium with a 1 M NaCl bath (middle), and in equilibrium with 2 M NaCl (right). (D) Micrographs of protein crystals grown using real-time feedback of observed aggregation. Crystals are from glucose isomerase (left), catalase (middle), and thaumatin (right). Scale bars are 100 μm.

Ferritin aggregation was found to be irreversible, and an experiment was set just below the solubility limit without prior aggregation. Interestingly, concentration back through the solubility limit resulted in the crystallization of all proteins except ferritin (Figure 3D), suggesting that the observed reversible precipitation indicates a microcrystalline aggregate rather than a denatured or amorphous solid phase.

The demonstrated integration of phase mapping and nanoliter volume crystallization provides a new tool for structural biology by enabling systematic crystallization trials of extremely scarce samples that otherwise would be intractable. The marriage of programmable microfluidic processing with high-density storage will find broad applications including membrane protein structural biology, proteomics, combinatorial chemistry, and cellomics.

Acknowledgment. This work was funded by NSERC of Canada (Discovery Grant) and the NIH (R21 R21EB005757).

Supporting Information Available: Fabrication protocols, details and video of device operation, solubility curves, crystallization protocols. This material is available free of charge via the Internet at http://pubs.acs.org.

References

(1) Thorsen, T.; Maerkl, S. J.; Quake, S. R. *Science* **2002**, 298.
(2) Zheng, B.; Tice, J.; Roach, L. S.; Ismagilov, R. F. *Angew. Chem., Int. Ed.* **2004**, *43*, 2508−2511.
(3) Song, H.; Ismagilov, R. F. *J. Am. Chem. Soc.* **2003**, *125*, 14613−14619.
(4) Hansen, C. L.; Classen, S.; Berger, J. M.; Quake, S. R. *J. Am. Chem. Soc.* **2006**, *128*, 3142−3143.
(5) Hansen, C. L.; Skordalakes, E.; Berger, J. M.; Quake, S. R. *Proc. Natl. Acad. Sci. U.S.A.* **2002**, *99*, 16531−16536.
(6) Hansen, C.; Sommer, M. O.; Quake, S. R. *Proc. Natl. Acad. Sci. U.S.A.* **2004**, *101*, 14431−14436.
(7) Sugiura, S.; Nakajima, M.; Iwamoto, S.; Seki, M. *Langmuir* **2001**, *17*, 5562−5566.
(8) Thorsen, T.; Roberts, R. W.; Arnold, F. H.; Quake, S. R. *Phys. Rev. Lett.* **2001**, *86*, 4163−4166.
(9) Tice, J. D.; Lyon, A. D.; Ismagilov, R. F. *Anal. Chim. Acta* **2004**, *507*, 73−77.
(10) Roach, L. S.; Song, H.; Ismagilov, R. F. *Anal. Chem.* **2005**, *77*, 785−796.

JA065855B